Initial Experience with Whole-Body Diffusion-Weighted Imaging in Oncological and Non-Oncological Patients

Marcos Vieira Godinho, M.D.[1]; Romulo Varella de Oliveira, M.D.[1]; Clarissa Canella, M.D., MSc[1]; Flavia Costa, M.D., MSc[1]; Thomas Doring, MSc[1]; Ralph Strecker, Ph.D.[2]; Romeu Cortes Domingues, M.D.[1]; Leonardo Kayat Bittencourt, M.D., MSc[1]

[1]*Clínica de Diagnóstico por Imagem, Rio de Janeiro, Brazil*
[2]*Siemens Healthcare, São Paulo, Brazil*

Background

Initially used as a diagnostic tool for acute stroke, over recent years diffusion-weighted imaging (DWI) has developed a growing role in the diagnosis and follow-up of diseases not only in extracranial pathologies, but also as a study of the whole body in systemic diseases, providing a steady increase of indications for the technique. With a growing elderly population worldwide and the highest incidence of oncologic illnesses, use of whole-body diffusion-weighted imaging (WBDWI) in this setting is evolving.

We initially used WBDWI for the already established indication in oncological patients with breast, prostate, gastrointestinal, hematological and other cancers, and then also decided to investigate its use in patients with auto-immune, inflammatory and infectious diseases.

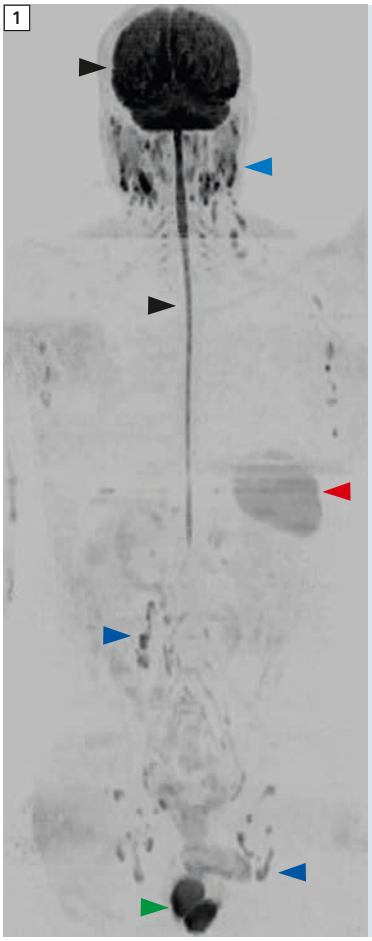

1 *b*800 WBDWI 3D MIP frontal view of a healthy 27-year-old control subject, with a past history of tonsillectomy and appendectomy, showing restricted diffusion in normal cervical, ileocecal and inguinal nodes (blue arrowheads), spleen (red arrowhead), CNS (black arrowheads) and testicles (green arrowhead). Also note different imaging contrast between stations.

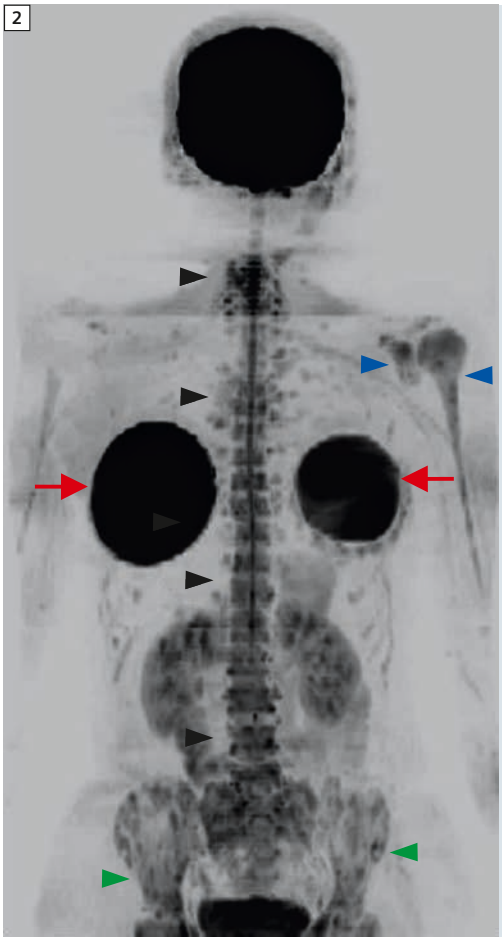

2 39-year-old female, diagnosis of breast cancer, bilateral mastectomy and mammoplasty, chemotherapy in course. 3D reconstruction from WBDWI in **(2A)**: multiple bone metastases along cervical, thoracic and lumbar spine (black arrowheads), pelvis (green arrowheads), left glenoid and humerus (blue arrowheads). Also note breast prostheses (red arrows).

The purpose of this article is to describe our examination technique, imaging protocols, interpretation of imaging findings and initial experience with oncological and non-oncological diseases, as well as the limitations of the study.

Methods

Since September 2011 we have recruited patients with oncological disease undergoing diagnostic or follow-up exams in our clinic with findings in conventional MRI suggestive of metastases, as well as patients with auto-immune or inflammatory systemic diseases and those with imaging findings that could be differential diagnosis for metastatic disease. In some cases the purpose was the staging of the disease before initial treatment, in other cases we did the follow-up of patients during therapy.

WBDWI was performed on a 1.5T clinical scanner (MAGNETOM Aera, Siemens Healthcare, Erlangen, Germany) recently installed in our center using two 18-channel body phase array coils together with the combined 20-channel Head/Neck coil. Patients were examined in supine position and four stations of axial free-breathing DWI with short tau inversion recovery (STIR) fat suppression were obtained using the following parameters: echo time (TE) 79 ms, repetition time (TR) 19000 ms, inversion time (TI) 180 ms, *b*-values 0 and 800 s/mm^2, read-out bandwidth 1502 Hz/pixel, 5 averages, field-of-view (FOV) 400 mm, slice thickness (SL) 5 mm, matrix size 128 × 128, voxel size 3.1 × 3.1 × 5.0 mm^3, acquisition time per station 7.17 min. The protocol also included four stations of axial T1-weighted (T1w) VIBE in- and opposed-phase images (TR 7.01 ms /TE1 2.38 ms /TE2 4.76 ms, FOV 450 mm, SL 5 mm, matrix 512 × 512, voxel size 0.9 × 0.9 × 5 mm^3) and axial T2-weighted (T2w) HASTE images with fat suppression STIR (TR 600 ms /TE 81 ms, FOV 420 mm, SL 5 mm, matrix size 256 × 256, voxel size 1.6 × 1.6 × 5 mm^3). Head, neck, chest, abdomen, pelvis and proximal thighs were studied. The four stations were composed inline, after the last station was acquired. No contrast media was administered and total duration of each exam was about 60 minutes.

So far, we have performed 4 exams with healthy controls, 9 exams with actual oncological patients (1 breast cancer, 1 small cell cancer with unknown primary site, 3 prostate cancers, 2 gastrointestinal neuroendocrine cancers, 1 plasmacytoma, 1 lymphoma) and 4 exams with non-oncological cases (1 prostatitis, 1 dermatopolymyositis, 1 spondyloarthritis, 1 chronic recurrent multifocal osteomyelitis).

Imaging findings

Our objective was to look for findings based on the principle that some neoplasms and their metastases have restricted diffusion because of their hypercellular nature. Inflammatory/infectious illnesses may also have foci of restricted diffusion along the body because some of them may produce abscesses. We always tried to detect lesions and to characterize their distribution. In other patients we also analyzed *b*0 images looking for the T2 shine-through effect, as explained further below.

For interpretation of WBDWI we used 'raw' data with inverted gray scale in *b*0 and *b*800 images, so lesions with restricted diffusion appeared as black foci in a white background (Figs. 4B and 6). In some cases, we also obtained the calculated *b*1400 images, improving the specificity of the findings, as in this case only lesions with real restricted diffusion were seen. Apparent Diffusion Coefficient (ADC) Maps were obtained for all patients and ADC values were measured. We also did three-dimensional maximum intensity projection (3D MIP) reconstructions using the Siemens composer tool in all cases and used T1w and STIR images for anatomical reference and fusion with WBDWI.

Control subjects

Before initiating the study with patients, we studied healthy subjects to test and adjust the protocols, to understand normal findings in the exams, considering the presence of imaging artifacts, problems with misregistration and intrinsic limitations of the study.

Normal brain tissue, spine, spleen and testicles had restricted diffusion, notably the latter. Even in control cases, small lymph nodes free of disease appeared with restricted diffusion, mainly in the neck, a finding which we consider as a limitation of the study (Fig. 1).

In some patients a mismatch between the head/neck and the thorax station, was observed. A problem most prominently visible in the 'broken spine' in sagittal MPR images and described by other authors before [1]. We also observed in some cases spatial variations in image intensity between the different stations which impaired the image interpretation of MPR images. It is worth to mention here that both the broken spine artifact and inhomogeneous signal can be corrected by using the new Diffusion Mode for Composing in software version *syngo* MR D13A.

We did not study the whole arms, because an increase in the size of the FOV would have been necessary, which could have reduced the resolution of the images.

Oncological patients

One of the most prominent features of the WBDWI were the study of metastatic bone disease, which was well depicted in most of the oncologic patients studied, with examples of all types of distribution (Figs. 2, 3 and 5–9), some confirmed by biopsy. In one patient with breast cancer the findings of bone scintigraphy were similar to that of WBDWI. In one of the patients (small cell cancer with unknown origin) when we compared the results of PET-CT scan with WBDWI, the last one showed a greater number of bone metastases (Figs. 7–9). The performance of WBDWI was even better in the case of diffuse bone marrow involvement when we analyzed it side by side with T1w in- and opposed-phase images and with fusion of both, to help in the differentiation of the lymphomatous infiltrate from hyperplastic red bone marrow (which could also present as black foci in the inverted gray scale of WBDWI), as there was no signal reduction in T1w opposed-phase compared with T1w in-phase images (Fig. 8). The reduced ADC values obtained in the lymphoma-

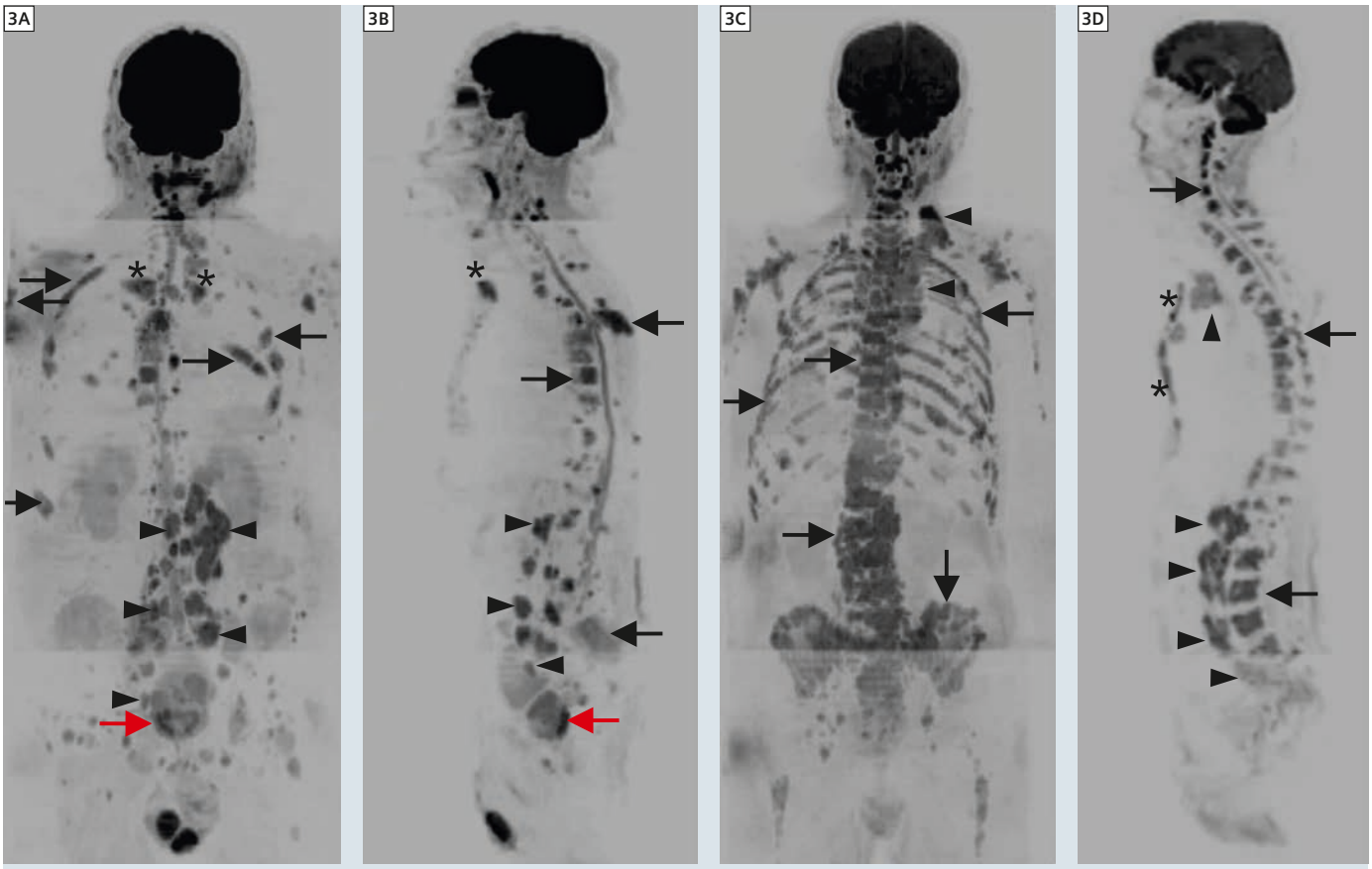

3 Two different patients with prostate cancer. Frontal **(3A)** and lateral views **(3B)** of *b*800 WBDWI 3D MIP of a 79-year-old male, recent diagnosis of prostate cancer during investigation of bone lesions: multiple bone metastases (black arrows), including lesions in the clavicles (asterisks) and enlarged pelvic and retroperitoneal lymph nodes (arrowheads). Also note markedly restricted diffusion in the prostate (red arrows). Frontal **(3C)** and lateral views **(3D)** of *b*800 WBDWI 3D MIP of an 84-year-old male, diagnosis of recurrent metastatic prostate cancer after prostatectomy: there are diffuse bone lesions (arrows) including metastases in the sternum (asterisk) and multiple enlarged pelvic and retroperitoneal lymph nodes as well as mediastinal and supraclavicular nodes (arrowheads), these last ones less common, characterizing advanced disease.

tous lesions also helped us to distinguish both.

Other kinds of metastatic spread could be shown, and enlarged lymph nodes were noted in patients with lymphoma, small cell and prostate cancers, the first one with disseminated nodal disease (Figs. 7 and 9), the second one with mediastinal nodal disease (Fig. 5) and the last ones with retroperitoneal spread (Fig. 3), corroborating the natural history of the diseases. One patient with relapsing prostate cancer had also enlarged mediastinal, axillary and supraclavicular lymph nodes, an uncommon finding most seen in advanced disease (Figs. 3C and 3D). However, the depiction of enlarged lymph nodes was not homogeneous along the body, because the performance of WBDWI to show metastatic lymph nodes in the mediastinum were worse in comparison with cervical, axillary, retroperitoneal and pelvic nodal spread, probably because of respiratory and cardiac motion artifacts and pulsation artifacts from thoracic arteries. In the patient with small cell cancer PET-CT showed more mediastinal disease than the WBDWI.

In one specific case, the patient came to our institution with shoulder pain and was submitted to MRI of the shoulder, showing lesions suspected for bone metastases. The study was complemented with WBDWI that showed much more bone lesions as well as retroperitoneal and pelvic nodal disease. The pattern and combination of bone and nodal disease, together with a mass with restricted diffusion infiltrating the prostate suggested the diagnosis of metastatic prostate cancer, confirmed by biopsy (Figs. 3A and 3B).

The detection of visceral metastases, mainly liver metastatic lesions, could be well done in 3 patients (1 small cell cancer and 2 neuroendocrine gastrointestinal tumors had multiple liver metastases), also showing us the natural history of the diseases. In the patient with small cell cancer most of the liver lesions had central necrosis without restriction of diffusion and a peripheral region of restricted diffusion (Fig. 5). No lesion was found in the central nervous system in any of the patients in WBDWI neither in other imaging sequences.

The patient with plasmacytoma was accompanied during the treatment (one DWI before and one after the beginning

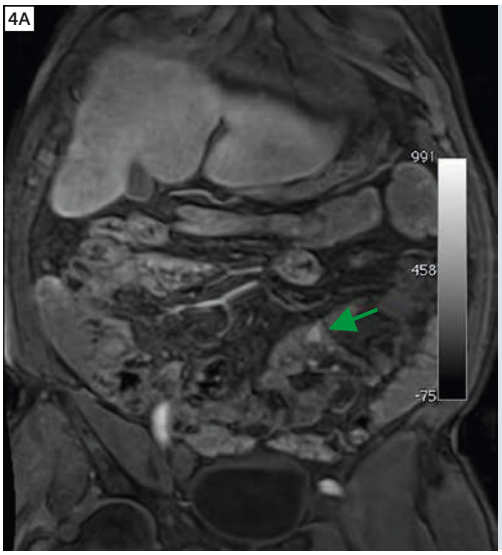

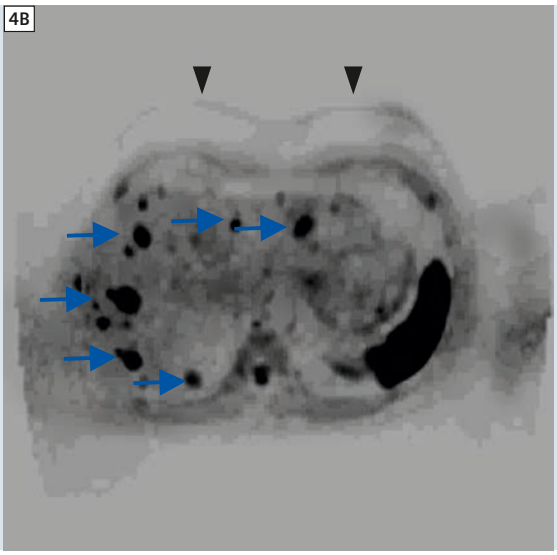

4 70-year-old male, carcinoid tumor of small bowel. Magnetic resonance enterography **(4A)**: small bowel lesion with contrast enhancement (green arrow). Axial *b*800 image **(4B)**: multiple liver metastases (blue arrows). The primary site was not well depicted in this case.

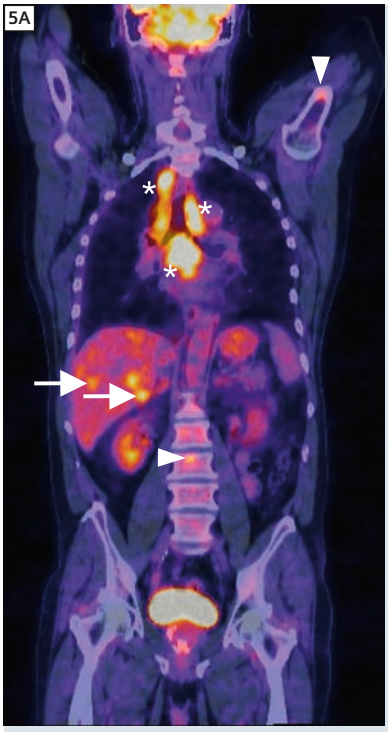

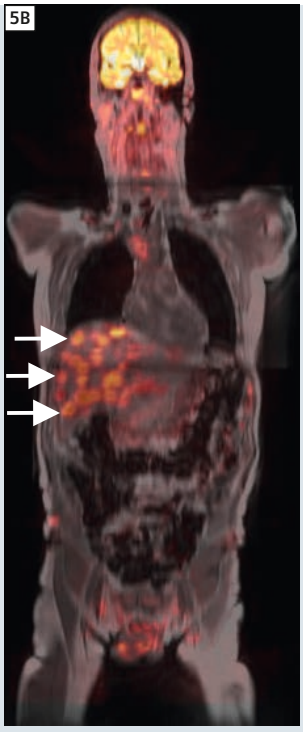

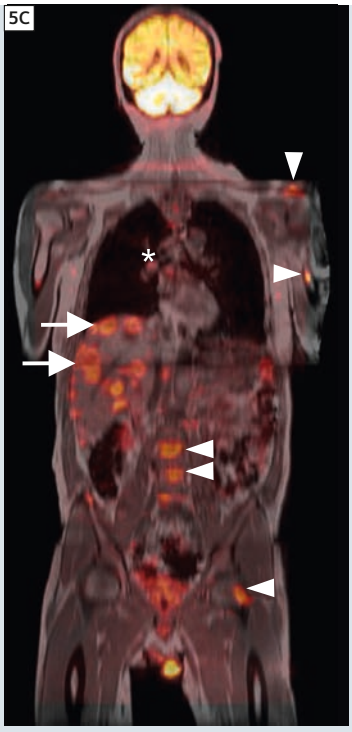

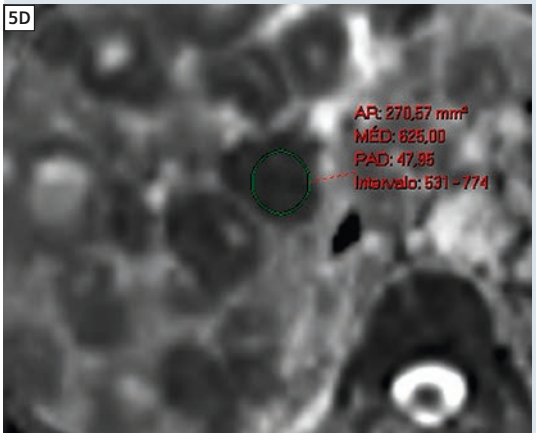

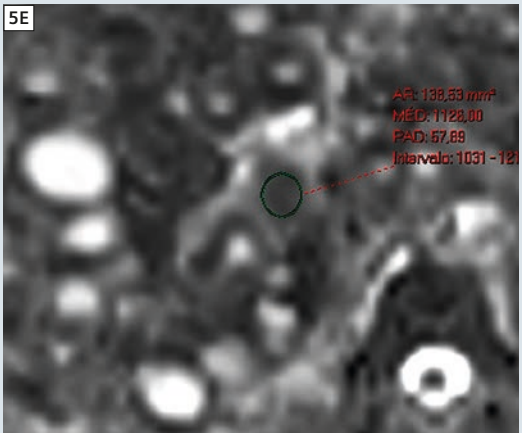

5 67-year-old male, investigating weight loss in the last six months. Biopsy of mediastinal enlarged lymph node has shown small cell cancer. No primary site was discovered. Reconstruction of PET-CT in coronal plane **(5A)** showing fluorodeoxyglucose uptake in liver (arrows) and bone lesions (arrowheads) and in enlarged mediastinal lymph nodes (asterisks). Fused T1w in-phase and *b*800 DWI coronal images **(5B and 5C)**: liver lesions with markedly restricted diffusion some with central necrosis (arrows), bone metastases (arrowheads) and mediastinal enlarged lymph nodes (asterisks). Bone lesions were better depicted in WBDWI, but comparison was compromised because WBDWI was done two months after PET-CT. Comparison between ADC values of one liver lesion in the first **(5D)** and second DWI **(5E)** two months after treatment: increasing ADC value of the lesion in follow-up image. Also note there are more areas of cystic/necrotic degeneration along the liver after initial treatment.

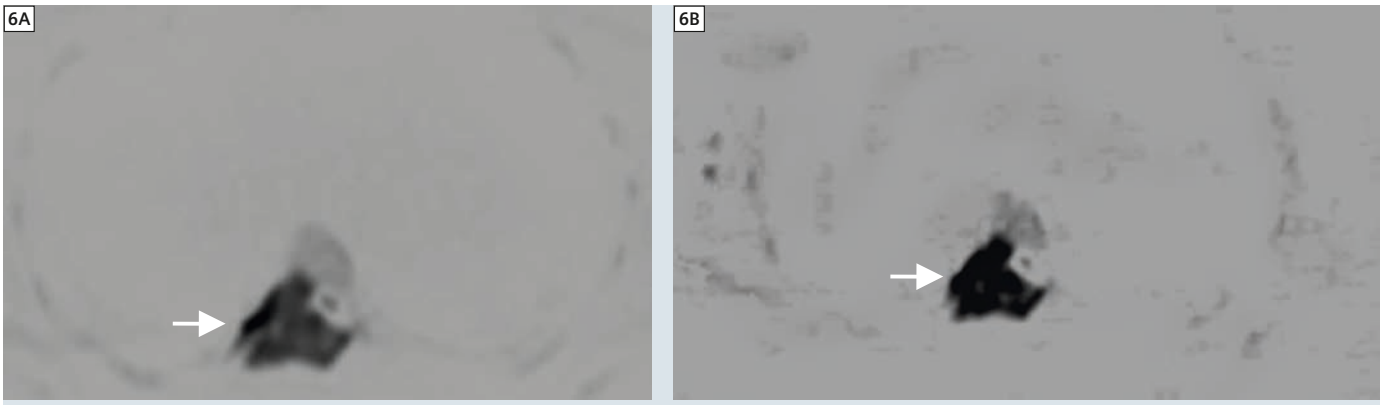

6 46-year-old female, dorsal thoracic pain. Axial *b*800 image **(6A)** and calculated *b*1400 image **(6B)** showing expansive lesion with markedly restricted diffusion in dorsal vertebral body (arrows). Biopsy revealed plasmacytoma.

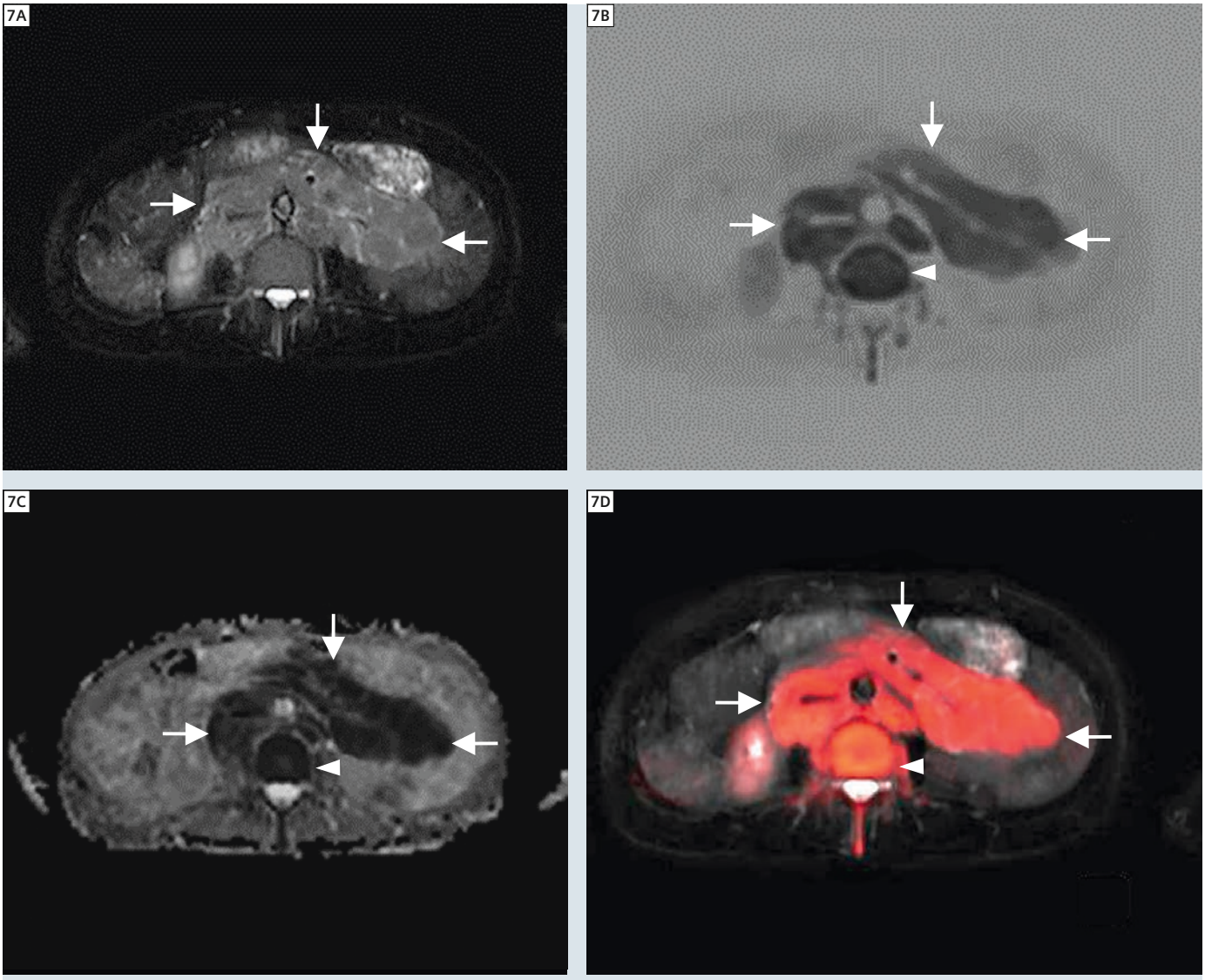

7 WBDWI of a 66-year-old female with recurrent lymphoma, presenting with diffuse enlarged lymph nodes and bone marrow infiltration. STIR **(7A)**, *b*800 DWI **(7B)**, ADC map **(7C)** and fused STIR and *b*800 DWI **(7D)**, showing conglomerate of retroperitoneal and mesenteric lymph node masses (arrows) and restricted diffusion in the bone marrow of a lumbar vertebra (arrowhead).

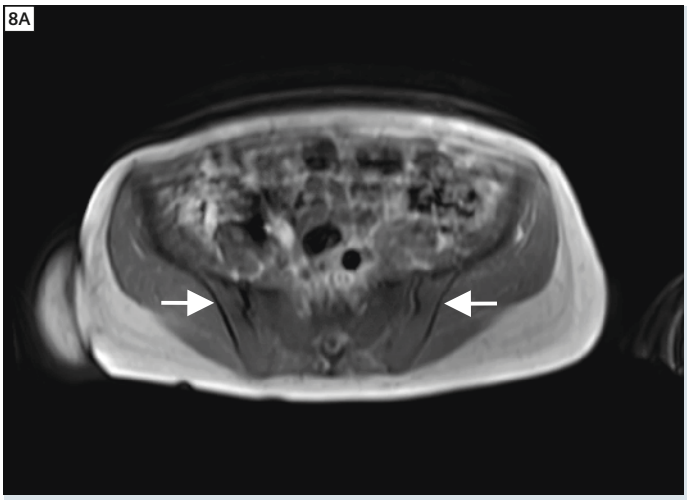

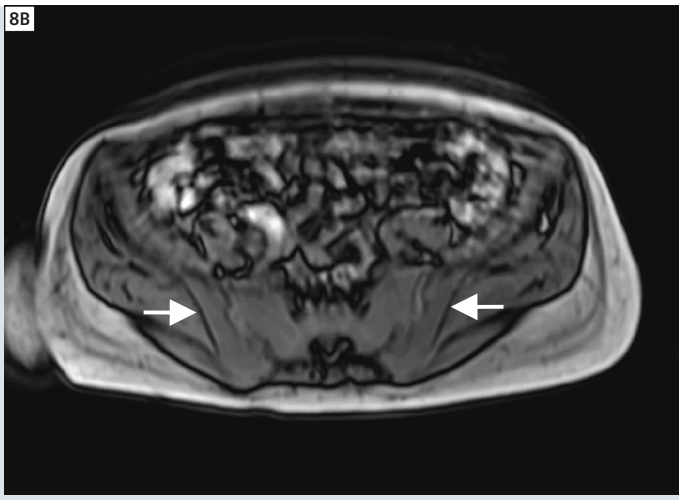

8 T1w in-phase **(8A)** and T1w opposed-phase **(8B)** of the bony pelvis in axial plane (same patient as in figure 7), showing diffuse bone marrow hypointensity, without signal reduction in T1w opposed-phase images, indicating tumoral infiltration instead of red marrow hyperplasia (confirmed by bone marrow biopsy).

9 Fused T1w in-phase and *b*800 DWI coronal images (same patient as in figure 7), showing diffuse bone marrow infiltration (arrowheads), conglomerate of retroperitoneal and mesenteric lymph node masses, and enlarged cervical, axillary, mediastinal, hepatic hilum, mesenteric, retroperitoneal, common iliac and external iliac lymph nodes (arrows). Note the spleen in left hypochondrium (asterisk).

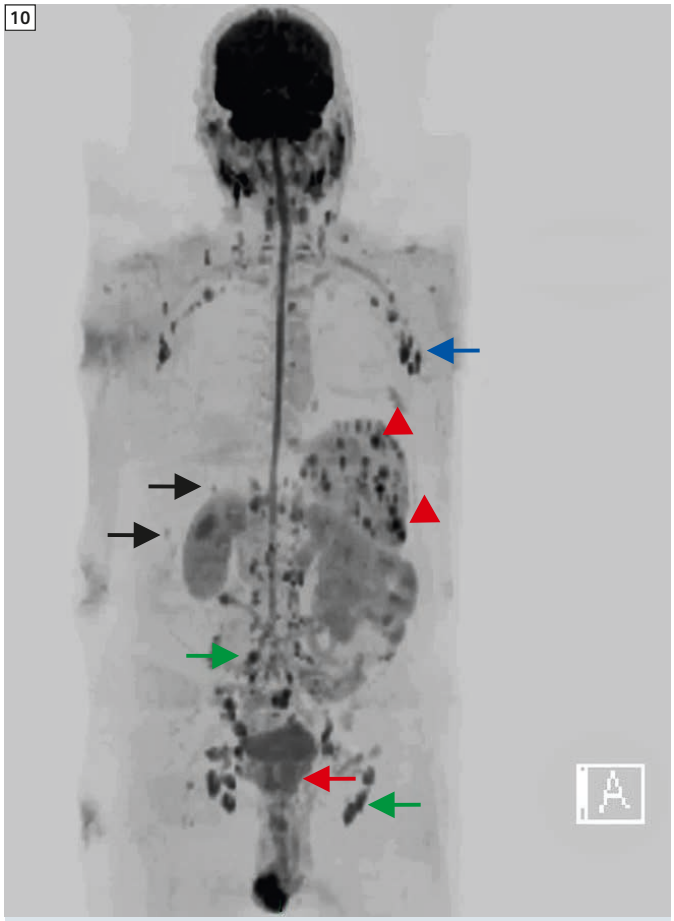

10 62-year-old male, HIV+, fever and malaise with prior negative prostate biopsy. 3D reconstruction from WBDWI showing prostatitis with slightly restricted diffusion in prostate (red arrow), associated with two tiny liver abscesses (black arrows), enlarged lymph nodes (green arrows) and multiple spleen abscesses with markedly restricted diffusion (red arrowheads).

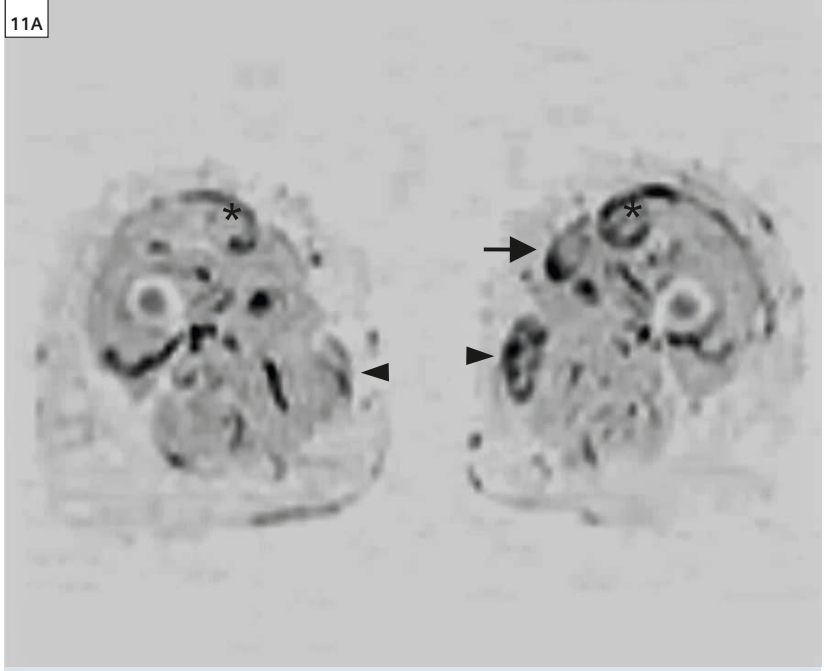

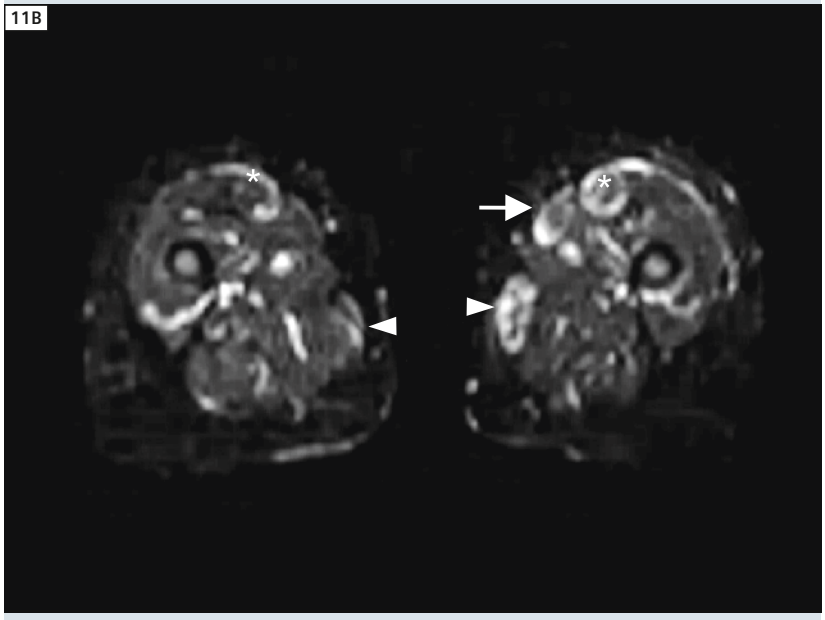

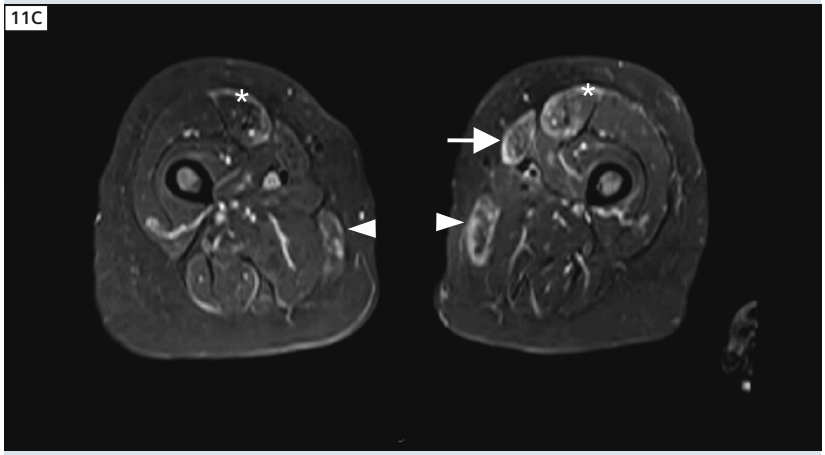

11 39-year-old female, diagnosis of dermatopolymyositis four months ago, treatment with corticosteroids, decreasing serum levels of muscle enzymes. Axial *b*0 images with inverted gray scale **(11A)** and standard gray scale **(11B)** and STIR images **(11C)**: edema in rectus femoris bilaterally (asterisks), left sartorius (arrow) and gracilis muscles (arrowheads) and in their respective aponeuroses.

of the treatment), where an increase of the ADC of the bone lesions was observed after two months of the first session of radiotherapy, with a subsequent improvement in the clinical symptoms. One of the patients with small cell tumor with unknown primary site was also followed up (one DWI before and one after the beginning of the treatment) and showed an increase in the ADC values in bone and liver lesions after one week of the second cycle of chemotherapy, also accompanied by clinical improvement (Fig. 5). Unlike other authors, we didn't use histogram analysis of the ADC values [2].

WBDWI beyond oncological applications

During the study a patient presented at our institution with fever and malaise investigating liver, splenic and nodal lesions one month after a negative biopsy for prostate cancer. He was submitted to a conventional MRI of the abdomen and pelvis and we complemented the exam with WBDWI. There were multiple lesions suggested of abscesses with central region presenting hypointense signal in T1w and hyperintense signal in STIR images with markedly restricted diffusion in the liver and notably in the spleen. We could also note axillary lymph nodes, as well as pelvic and retroperitoneal enlarged lymph nodes, the latter with apparent central areas of abscess formation on conventional images. There were also foci with slightly restricted diffusion in the prostate (Fig. 10). The type and pattern of distribution of the lesions suggested the diagnosis of prostatitis with septic foci to lymph nodes and solid viscera, which was confirmed by laboratory exams. Adequate antibiotics were administered and there was clinical improvement of the patient initially. During the investigation of prostatitis it was also discovered the patient was HIV positive with Acquired Immunodeficiency Syndrome, which could have helped in the spread of the septic disease.

In rheumatic patients, we mostly used the T2 shine-through effect of WBDWI in the interpretation of images. The patient with dermatopolymyositis had decreas-

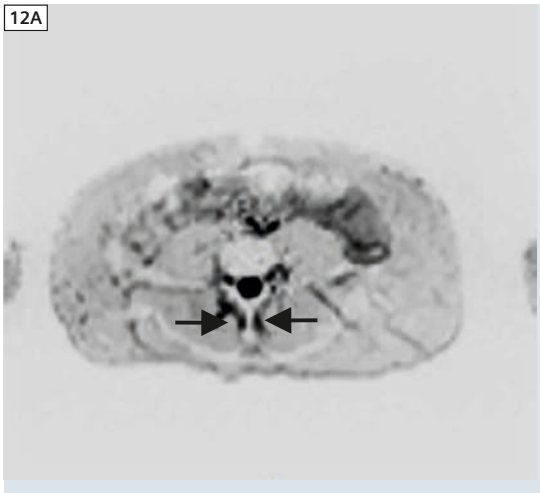

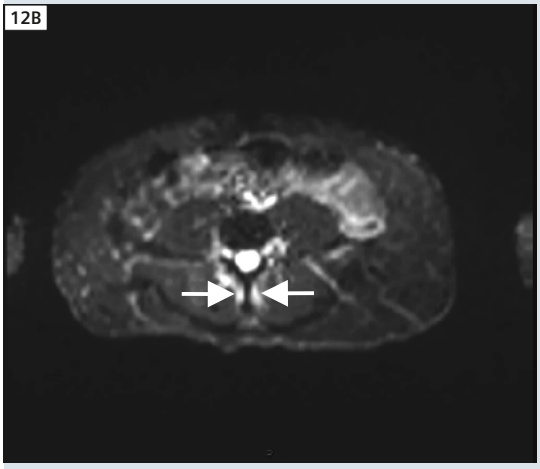

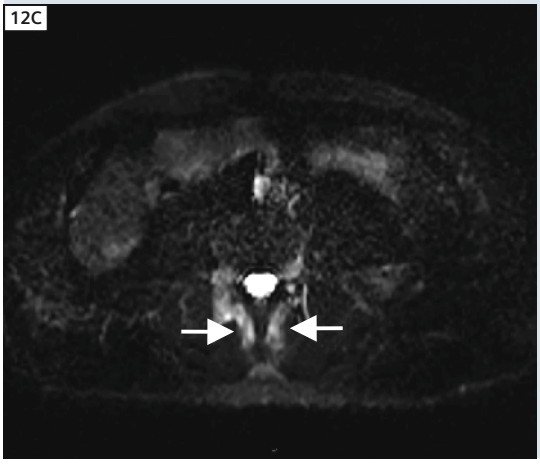

12 34-year-old male, diagnosis of spondyloarthritis, significant pain and movement restriction of the lumbar spine. Axial *b*0 images with inverted gray scale **(12A)** and standard gray scale **(12B)** and STIR images **(12C)**: edema near the spinous process of a lumbar vertebra, configuring enthesitis (arrows). The study was complemented with composed STIR images in sagittal plane **(12D)** depicting discrete edema in interspinal ligaments in lumbar spine (arrowheads).

ing serum titles of muscle enzymes and had edema predominantly in rectus femoris, sartorius and gracilis muscles and their aponeuroses in the thighs (Fig. 11). In the patient with spondyloarthritis, enthesitis near the spinous processes of lumbar spine and in interspinal ligaments could be well depicted (Fig. 12), a finding described in the literature [3]. Chronic recurrent multifocal osteomyelitis (CRMO) is an autoinflammatory disorder of children and young adults that is characterized by non-bacterial osteomyelitis presenting with multifocal bone pain secondary to sterile osseous inflammation, with a relapsing and remitting course. In the study of the patient with CRMO we also included in the protocol a station for the distal thighs and legs. This patient had marked bilateral edema in metaphyses around the ankles and the knees adjacent to the growth plate, this last one being the most common location of the disease in the tubular

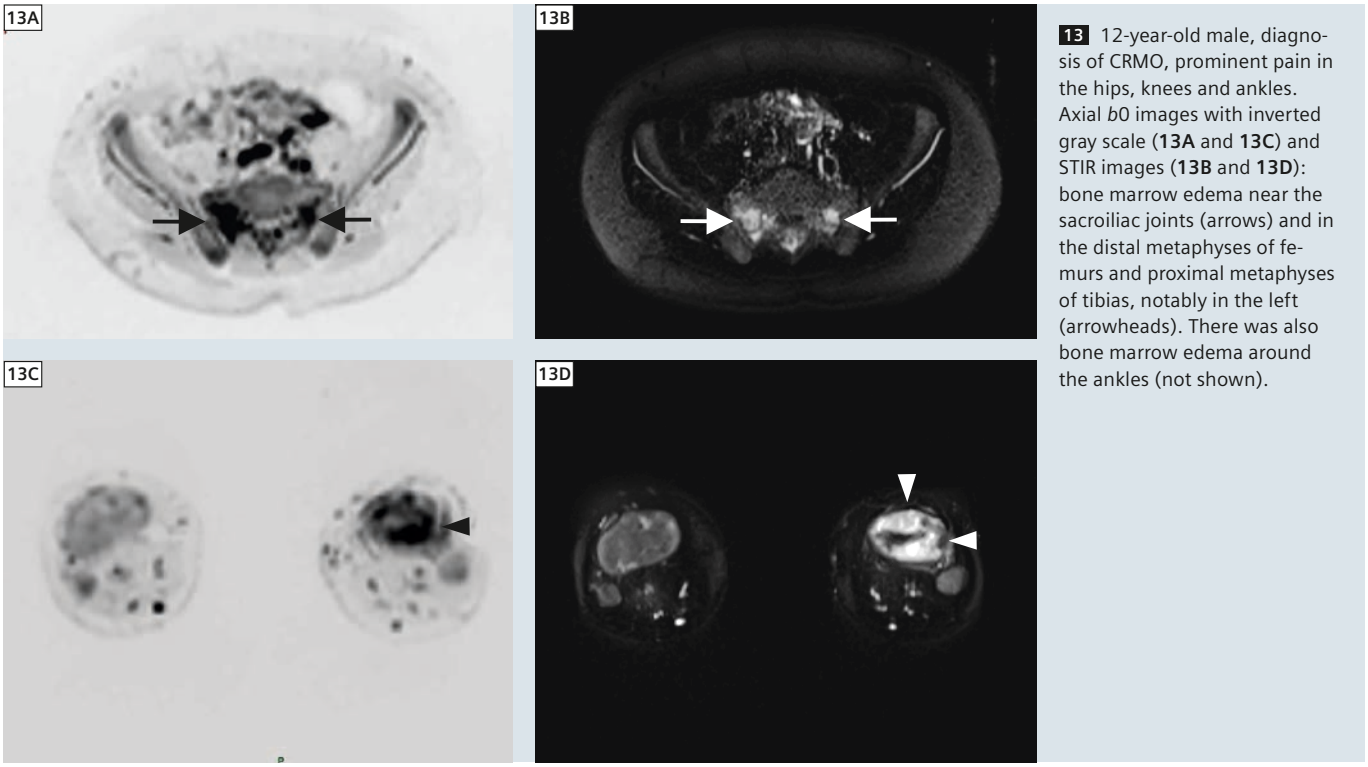

13 12-year-old male, diagnosis of CRMO, prominent pain in the hips, knees and ankles. Axial *b*0 images with inverted gray scale (**13A** and **13C**) and STIR images (**13B** and **13D**): bone marrow edema near the sacroiliac joints (arrows) and in the distal metaphyses of femurs and proximal metaphyses of tibias, notably in the left (arrowheads). There was also bone marrow edema around the ankles (not shown).

bones according to the literature [4], and prominent edema in the sacrum near the sacroiliac joints, a finding less common (Fig. 13). In rheumatic diseases, *b*0 images had a similar performance in comparison with STIR images to detect muscle and bone marrow edema, as well as in the detection of enthesopathy. The *b*800 images were not helpful in these cases, because the lesions had no real restricted diffusion.

Conclusion

WBDWI may play an important role in the near future for the detection of visceral and mostly bone metastases from many types of cancer.
The method is also promising in the demonstration of a visual notion of the disease as a whole in some auto-immune and inflammatory illnesses, probably helping in the assessment of their severity. One of our colleagues is studying a larger number of patients with chronic recurrent multifocal osteomyelitis (CRMO) using WBDWI, so that we soon may have more answers about the advantages and disadvantages of WBDWI in these cases. We have not studied other possible indications of WBDWI, for example the assessment of bone marrow features in patients with other hematological non-neoplastic conditions, such as sickle cell disease and thalassemia, which is certainly a large field to be explored. Our center is not an academic institution and we didn't enroll patients in a randomized and double-blind fashion. So far, the exact role of WBDWI in the oncological and non-oncological setting and its sensitivity, specificity and accuracy in comparison with other exams (e.g. bone scintigraphy, PET-CT, PET-MR) must be accessed by large clinical trials.

References

1 Koh DM, Blackledge M, Padhani AR, Takahara T, Kwee TC, Leach MO, Collins DJ. Whole-Body Diffusion-Weighted MRI: Tips, Tricks, and Pitfalls. AJR. 2012 Aug; 199:252-262.
2 Padhani AR, Koh DM, Collins DJ. Whole-Body Diffusion-weighted MR Imaging in Cancer: Current Status and Research Directions. Radiology. 2011 Dec; 261(3): 700-718.
3 Hermann KGA, Althoff CE, Schneider U, Zühlsdorf S, Lembcke A, Hamm B, Bollow M. Spinal Changes in Patients with Spondyloarthritis: Comparison of MR Imaging and Radiographic Appearances. RadioGraphics. 2005; 25:559-570.
4 Khanna G, Sato TSP, Ferguson P. Imaging of Chronic Recurrent Multifocal Osteomyelitis. RadioGraphics. 2009; 29:1159-1177.

Marcos Vieira Godinho

Leonardo Kayat Bittencourt

Contact
Marcos Godinho
Clínica de Diagnóstico por Imagem
Rio de Janeiro
Brazil
mgodinho25@yahoo.com.br